

# Anatomical factors influencing patellar tracking in the unstable patellofemoral joint

Rahul Biyani · John J. Elias · Archana Saranathan ·  
Hao Feng · Loredana M. Guseila ·  
Melanie A. Morscher · Kerwyn C. Jones

Received: 21 February 2014 / Accepted: 16 July 2014 / Published online: 26 July 2014  
© Springer-Verlag Berlin Heidelberg 2014

## Abstract

**Purpose** The current study was performed to relate anatomical parameters to in vivo patellar tracking for pediatric patients with recurrent patellar instability.

**Methods** Seven pediatric patients with recurrent patellar instability that failed conservative treatment were evaluated using computational reconstruction of in vivo patellofemoral function. Computational models were created from high-resolution MRI scans of the unloaded knee and lower-resolution scans during isometric knee extension at multiple flexion angles. Shape matching techniques were applied to replace the low-resolution models of the loaded knee with the high-resolution models. Patellar tracking was characterized by the bisect offset index (lateral shift) and lateral tilt. Anatomical parameters were characterized by the inclination of the lateral ridge of the trochlear groove, the tibial tuberosity–trochlear groove distance, the Insall–Salvati index and the Caton–Deschamps index. Stepwise multivariable linear regression analysis was used to relate patellar tracking to the anatomical parameters.

**Results** The bisect offset index and lateral tilt were significantly correlated with the lateral trochlear inclination ( $p \leq 0.002$ ) and TT–TG distance ( $p < 0.05$ ), but not the Insall–Salvati index or the Caton–Deschamps index. For both the bisect offset index and lateral tilt, the standardized beta coefficient, used to identify the best anatomical predictors of tracking, was larger for the lateral trochlear inclination than the TT–TG distance.

**Conclusion** For this population, the strongest predictor of lateral maltracking that could lead to patellar instability was lateral trochlear inclination.

**Level of evidence** Diagnostic study, Level II.

**Keywords** Patellar instability · Patellar tracking · Trochlear dysplasia · Tibial tuberosity–trochlear groove distance

## Introduction

Patellar instability is a common and disabling condition in the pediatric population. Females ranging in age from 10 to 17 are at the highest risk for lateral patellar dislocation [17], with dislocation the most common acute knee disorder in children and adolescents [26]. An initial dislocation commonly leads to recurrent instability, as the redislocation rate following conservative treatment can be greater than 40 % [8, 9, 24] and up to 60 % in patients younger than 15 years of age [6]. Numerous surgical options are available to treat recurrent instability, such as medial patellofemoral ligament reconstruction and tibial tuberosity realignment, with the choice of approach based on factors including the history, anatomy and age of the patient.

Previous imaging studies have identified several anatomical parameters that contribute to patellar instability,

---

R. Biyani · J. J. Elias  
Department of Orthopedic Surgery, Akron General Medical  
Center, Akron, OH, USA

J. J. Elias (✉) · A. Saranathan · H. Feng · L. M. Guseila  
Department of Research, Akron General Medical Center,  
1 Akron General Avenue, Akron, OH 44307, USA  
e-mail: john.elias@akrongeneral.org

H. Feng  
Department of Mechanical Engineering, University of Akron,  
Akron, OH, USA

M. A. Morscher · K. C. Jones  
Department of Orthopedic Surgery, Akron Children's Hospital,  
Akron, OH, USA

and additional studies have focused on the relationship between tracking and anatomy. Anatomical parameters that have been related to patellar instability include the tibial tuberosity–trochlear groove (TT–TG) distance [1, 2, 28], which is used to assess the lateral force acting on the patella from the patellar tendon, and the Insall–Salvati and Caton–Deschamps indices [7, 34], which are measures of patella alta. Parameters related to trochlear dysplasia, such as an increased sulcus angle, a decreased lateral trochlear inclination and assessment based on the Dejour classification, have also been associated with patellar instability [1, 7, 18, 22, 26]. Imaging studies performed with asymptomatic subjects and subjects with patellofemoral pain with the knee loaded at various flexion angles have associated Insall–Salvati index [27, 33, 36], Caton–Deschamps index [27], lateral trochlear inclination [33] and other parameters related to trochlear dysplasia [35] with an increased lateral shift and tilt of the patella.

Based on the previous literature, an elevated TT–TG distance, trochlear dysplasia and patella alta are considered the primary anatomical conditions leading to lateral patellar maltracking and instability episodes. To date, these anatomical contributors to lateral maltracking have not been evaluated simultaneously for subjects with patellar instability. The current study was performed to evaluate the influence of all three anatomical conditions on patellar tracking in pediatric subjects with recurrent patellar instability. The goal was to quantify the relative contributions of the three types of pathology to maltracking in order to identify the primary anatomical factors contributing to recurrent instability.

## Materials and methods

The current study utilized computational reconstruction of in vivo function to characterize the relationship between anatomy and patellar tracking. Seven subjects, six of them female, with recurrent patellar dislocations were included in the study. The average age (standard deviation) for the subjects was 16 (3) years. The physeal status for the distal femur and proximal tibia was open for two subjects, closing for one and closed for four. All subjects had at least two traumatic episodes of complete excursion of the patella from the trochlear groove and had failed an interval of bracing and physical therapy of at least 3 months. Subjects that had previous injuries or surgeries to the affected knee were excluded from the study group.

Computational models were created from MRI scans (3.0 T, Magnetom Skyra, Siemens, Malvern, PA) to represent the effected knee of each subject in an unloaded condition and with the knee flexed and loaded at multiple flexion angles. The scans were acquired in a single session

lasting approximately 1 h. A high-resolution scan was performed first with the effected knee extended and unloaded. The flexed and loaded scans were performed with an MRI-compatible load frame that used an elastic band to apply force to the foot along the axis of the scanner. The deformation of the band was adjustable, with the force applied as a function of displacement calibrated using a hand-held force transducer (Force One FDIX, Wagner Instruments, Greenwich, CT). Due to variations in patellar stability and pain, each patient self-selected the largest resistance that could be comfortably maintained for the duration of a scan. Resistance levels ranged from 60 to 85 N and were selected in a separate room prior to scanning. The flexed scans were initiated at the largest angle that could be accommodated within the bore of the MRI scanner (32°–58°), with additional scans as the flexion angle was decreased to the lowest that the patient could hold for the duration of a scan (–20°–14°). Five to seven scans were analyzed for each patient. At low flexion angles, patients were asked to engage the quadriceps without locking the knee.

Scanning methods were adapted from previous publications [4, 25]. The high-resolution scan of the unloaded knee used a knee coil (Tx/Rx CP extremity coil, Siemens, Malvern, PA) for image acquisition. Proton density-weighted images were acquired with a turbo spin echo pulse sequence in the sagittal plane. The other parameters included a field of view of 16 cm, 512 × 256 matrix, in plane resolution of 0.3 mm and slice thickness of 1.5 mm. Scans were acquired in approximately 8 min. The low-resolution scans of the flexed knee were acquired in approximately 30 s using a flexible extremity coil (Large 4-Channel Flex Coil, Siemens). A T1-weighted turbo spin echo sequence was used to acquire images in the sagittal plane. The other parameters included a field of view of 16 cm, 256 × 256 matrix, in plane resolution of 0.6 mm, slice thickness of 2 mm and slice spacing of 4 mm. Minimizing the time for the low-resolution scan was necessary due to the limited ability to resist external loads with the symptomatic knee.

Reconstruction of models from the imaging data and shape matching techniques were used to create a representation of each knee at each flexion angle. The high-resolution scan provided images for reconstruction of the femur, tibia and patella, as well as the cartilage within the trochlear groove and on the patella. The low-resolution scans performed at multiple flexion angles with the knee loaded provided images to reconstruct models of the bones, without cartilage. Semi-automated tracing algorithms were used to create computational graphical models from scanned images (3D Doctor, Able Software Corp, Lexington, MA). For each subject, the models from each scan of a flexed knee were aligned to the femur including cartilage from the high-resolution scan with the iterative closest point

**Fig. 1** Shape matching techniques are used to replace the reconstructed bones from low-resolution scans representing the flexed and loaded knee with bones including cartilage from a high-resolution scan of the extended, unloaded knee

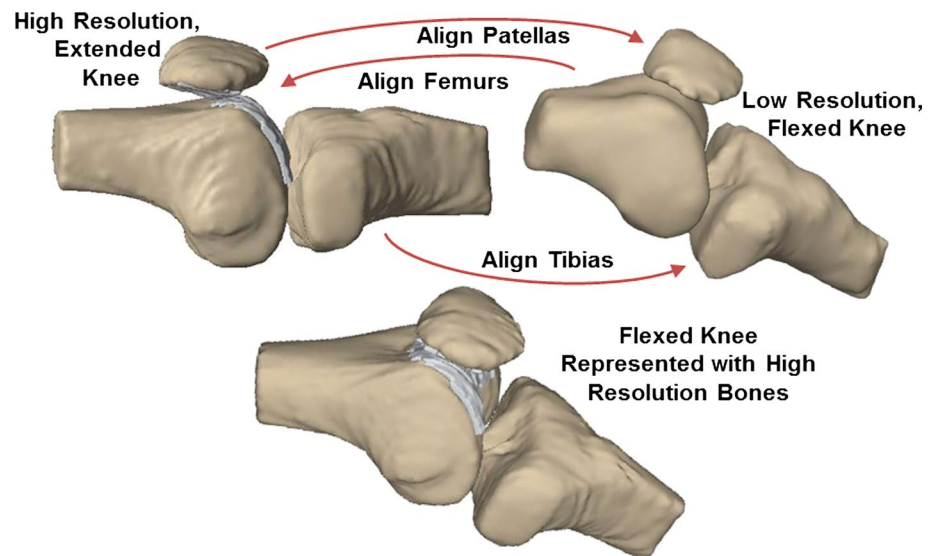
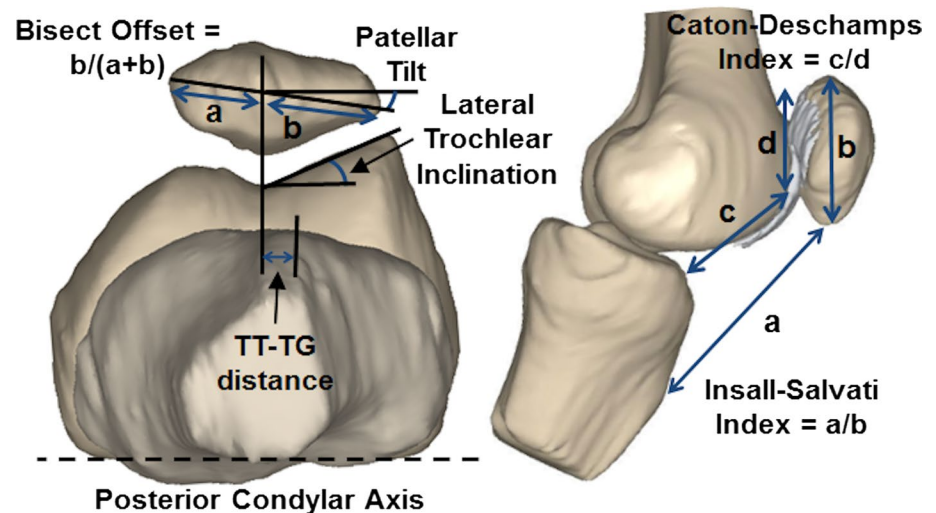


**Fig. 2** Patellar tracking is characterized by the bisect offset index (measure of lateral shift) and patellar lateral tilt. Trochlear dysplasia and the lateral force applied by the patellar tendon are characterized by the lateral trochlear inclination and TT–TG distance, respectively. Patella alta is characterized by the Caton–Deschamps index and Insall–Salvati index



algorithm [3]. A computational algorithm (Matlab, Mathworks, Natick, MA) aligned the femurs based on points within and surrounding the trochlear groove to focus on the region of patellofemoral articulation (Fig. 1). The patella, including cartilage, and the tibia from the high-resolution scan were then aligned to the respective bones at each flexion angle from the low-resolution scans. For the patella, the alignment was based on points on the posterior surface of the patella to focus on the region of patellofemoral articulation. For the tibia, the alignment included the length of the proximal tibia common to both models.

Analysis of the models focused on relating anatomical parameters to patellar tracking. Patellar tracking was characterized in terms of the bisect offset index and patellar lateral tilt (Fig. 2) [27, 36]. The bisect offset index characterizes lateral shift of the patella by the portion of the patellar width lateral to the deepest point of the trochlear

groove. The lateral tilt measures the angle between a line along the medial–lateral axis of the patella and a line along the posterior condyles of the femur. The anatomical parameters included the TT–TG distance, characterized by the lateral distance from the deepest point of the trochlear groove to the patellar tendon attachment on the tibial tuberosity [1, 2, 28]. Trochlear dysplasia was characterized based on the lateral trochlear inclination, the angle of the lateral ridge of the trochlear groove with respect to the posterior condyles [31–33]. Patella alta was characterized with two parameters, the Caton–Deschamps and Insall–Salvati indices. The Caton–Deschamps index is the ratio of the distance from distal point of the patellar cartilage to the anterior–superior border of the tibia to the articular length along the patella [7, 27]. The Insall–Salvati index is the ratio of the length of the patellar tendon to the total length of the patella [7, 27].

The reconstructed models were graphically manipulated to perform the analysis at each flexion angle. A proximal–distal axis parallel to the most posterior aspect of the patella was established within the high-resolution model of the patella. The knee was rotated to bring this axis perpendicular to the plane of evaluation. A second rotation aligned the most posterior points on the femoral condyles horizontally (Fig. 2). The medial–lateral axis of the high-resolution model of the patella was identified from the most medial and lateral points on the patella. The length of the articular surface on the patella was determined from points marking the proximal and distal edges of the cartilage, and the total length was determined from the most proximal and distal points on the patella. The anterior–superior border of the tibia was identified on the high-resolution model of the tibia, and the center of the tibial tuberosity was identified based on reconstruction of the patellar tendon attachment at the tibia from the MRI scan. The deepest point of the trochlear groove and the most prominent point of the lateral trochlear ridge were quantified for each knee flexion angle using an automated algorithm. To select points within the trochlear groove that were engaged with the patella, the most prominent lateral point was taken from the region of overlap of the cartilage on the femur and patella, or the closest point if no overlap was detected, plus 5 mm in the proximal and distal directions. The deepest point of the trochlear groove was identified within the same axial slice as the most prominent point on the lateral trochlear ridge to characterize the lateral trochlear inclination opposing lateral translation.

To assess the accuracy of the reconstruction technique, anatomical and tracking measures were compared to the same measurements based on only imaging data without additional shape matching. For six knees, one low-resolution reconstruction with the knee flexed and loaded that provided sufficient resolution of the landmarks for characterization of the output was identified. All of the output measures were quantified from the low-resolution model. The root mean square error between the output from the high-resolution models with shape matching and the low-resolution models was 1.2° and 0.04 for the lateral tilt and bisect offset index, respectively. The root mean square error for the lateral trochlear inclination, TT–TG distance, Caton–Deschamps index and Insall–Salvati index was 1.3°, 1.1 mm, 0.04 and 0.1, respectively. The intraclass correlation coefficient (ICC) for the repeated measurements was greater than 0.9 for all parameters, except the Insall–Salvati index, for which the ICC was 0.82.

#### IRB Approval

The study was approved by the IRB of Akron Children's Hospital (ID #110908). A parent or guardian of each

subject provided informed consent prior to enrollment in the study, with a separate assent provided by each patient.

#### Statistical analysis

Statistical analysis focused on the relationship between anatomy and tracking. Correlation of bisect offset index and patellar lateral tilt with the anatomical parameters was evaluated using stepwise multivariable linear regression analyses (Minitab 16, Minitab, State College, PA), with only the parameters that significantly ( $p < 0.05$ ) contribute to the regression retained in each analysis. Standardized beta coefficients, which quantify the relative predictive values of the independent variables, identified the best anatomical predictors of bisect offset index and lateral tilt for significant multivariable regressions. The square of the correlation coefficient,  $r^2$ , was also quantified for each variable, as well as the combination of multiple variables. The analyses were performed grouping the data for all knees at all flexion angles and considering only the data with the knee at the most extended position, since measures of patellar tilt and bisect offset index are typically largest at full extension for subjects with patellofemoral disorders [13, 14, 29, 33]. Considering all data for all subjects, a power analysis for multivariable linear regression indicated a variable increasing  $r^2$  by 0.1 in a regression with a total of  $r^2$  of 0.5 could be evaluated at a power of 0.8 and a significance of 0.05 (G\*Power 3.1.9 [15]). Considering only data at the most extended position for each subject, regression lines with an  $r^2$  of 0.64 could be evaluated at a power of 0.8 and a significance of 0.05.

#### Results

Over all flexion angles, bisect offset index and patellar lateral tilt tended to be negatively correlated with the lateral trochlear inclination (Figs. 3, 4) and positively correlated with the TT–TG distance (Figs. 5, 6). For the bisect offset index and lateral tilt, multivariable linear regression showed significant correlations with lateral trochlear inclination ( $p \leq 0.002$ ) and TT–TG distance ( $p < 0.05$ ), with an adjusted  $r^2$  for the combination of the two anatomical parameters of 0.70 and 0.46, respectively (Table 1). For the bisect offset index, the magnitude of the standardized beta coefficient for the lateral trochlear inclination was more than three times the value for the TT–TG distance. For lateral tilt, the standardized beta coefficient magnitude for the lateral trochlear inclination was 60 % larger than for the TT–TG distance. No significant relationships with the tracking parameters were identified when the Caton–Deschamps index or the Insall–Salvati index were added to the multivariable regression analysis (Table 1).

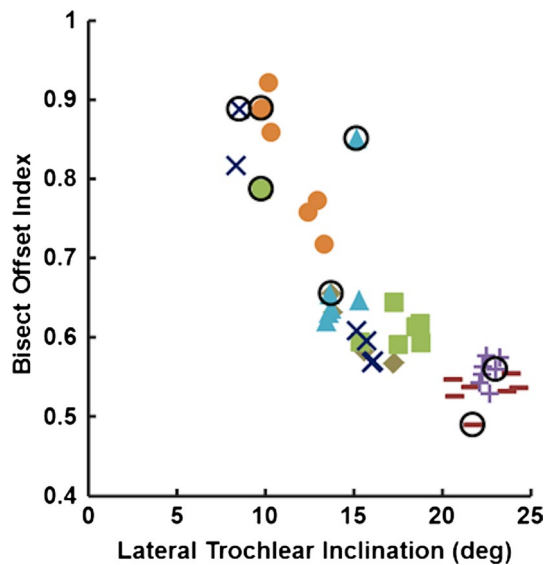


**Fig. 3** Variation in the bisect offset index with the lateral trochlear inclination for all subjects at all flexion angles. The seven subjects are represented by seven *separate symbols*. Circled data points represent the most extended position for each subject

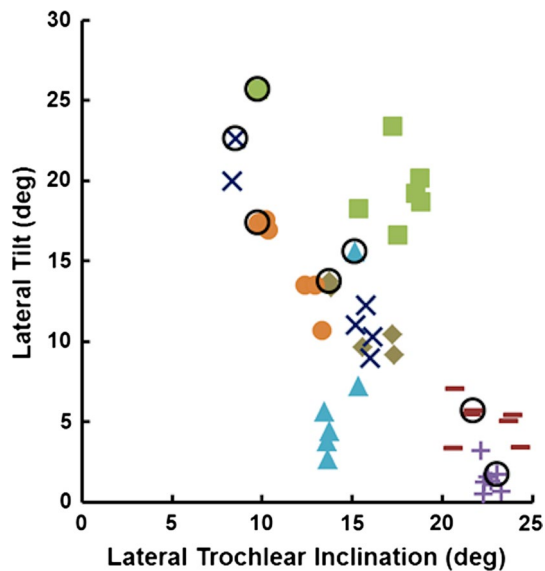


**Fig. 4** Variation in the patellar lateral tilt with the lateral trochlear inclination for all subjects at all flexion angles. The seven subjects are represented by seven *separate symbols*. Circled data points represent the most extended position for each subject

At the most extended flexion angle, patellar tilt and bisect offset index were correlated with only the lateral trochlear inclination. In the most extended position, the TT–TG distance ranged from 1 to 24 mm, with an average of 11 (8) mm. The lateral trochlear inclination ranged from 9° to 23°, with an average of 15 (6)°. The

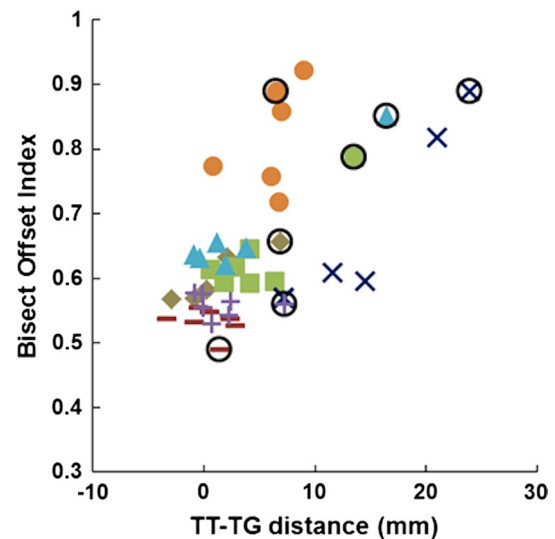


**Fig. 5** Variation in the bisect offset index with the TT–TG distance for all subjects at all flexion angles. The seven subjects are represented by seven *separate symbols*. Circled data points represent the most extended position for each subject

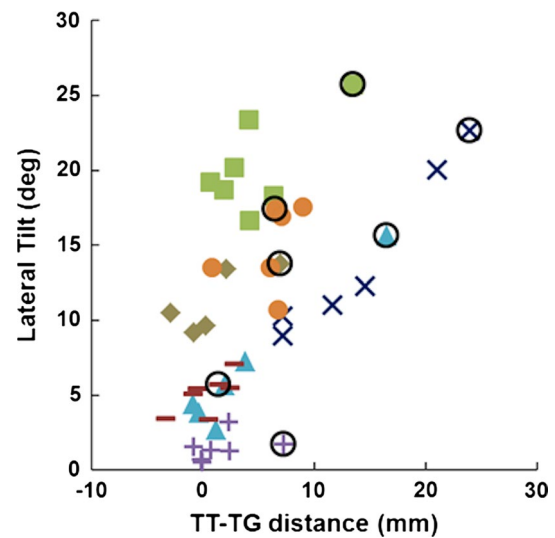


**Fig. 6** Variation in the patellar lateral tilt with the TT–TG distance for all subjects at all flexion angles. The seven subjects are represented by seven *separate symbols*. Circled data points represent the most extended position for each subject

Insall–Salvati index ranged from 1.0 to 1.4, with an average of 1.2 (0.1), and the Caton–Deschamps index ranged from 0.7 to 1.1, with an average of 1.0 (0.1). Bisect offset index and lateral tilt were both significantly correlated with lateral trochlear inclination ( $p \leq 0.01$ ), with  $r^2$  values of 0.76 and 0.90, respectively (Table 2). No significant relationships were established for the other anatomical parameters (Table 2).



**Table 1** Results of regression analyses considering all subjects at all flexion angles

	Bisect offset index			Patellar lateral tilt		
	Total	LTI	TT–TG	Total	LTI	TT–TG
Multi-variable regression for lateral trochlear inclination, TT–TG distance						
<i>p</i> values	<0.001	<0.001	0.04	<0.001	0.002	0.04
<i>r</i> <sup>2</sup>	0.70	0.68	0.41	0.46	0.43	0.34
β coefficient		−0.69	0.22		−0.48	0.30
	IS index		CD index	IS index		CD index
IS index, CD index added to multivariable regression						
<i>p</i> values	n.s.		n.s.	n.s.		n.s.
<i>r</i> <sup>2</sup>	0.001		0.13	0.04		0.15

LTI lateral trochlear inclination, TT–TG tibial tuberosity–trochlear groove, IS Insall–Salvati, CD Caton–Deschamps, n.s. not significant

**Table 2** Results of regression analyses considering all subjects at most extended position

	Bisect offset index				Patellar lateral tilt			
	LTI	TT–TG	IS index	CD index	LTI	TT–TG	IS index	CD index
Independent regressions for LTI, TT–TG distance, IS index, CD index								
<i>p</i> values	0.01	n.s.	n.s.	n.s.	0.001	n.s.	n.s.	n.s.
<i>r</i> <sup>2</sup>	0.76	0.52	0.04	0.01	0.90	0.37	0.002	0.001

LTI lateral trochlear inclination, TT–TG tibial tuberosity–trochlear groove, IS Insall–Salvati, CD Caton–Deschamps, n.s. not significant

## Discussion

The most important finding of this study was that trochlear dysplasia is the primary parameter influencing patellar tracking in pediatric patients being treated for recurrent instability, with TT–TG distance a secondary factor. Trochlear dysplasia, in the form of low lateral trochlear inclination, combined with TT–TG distance to be significantly correlated with bisect offset index and patellar lateral tilt over all subjects at all flexion angles. The standardized coefficients indicated that the relationship was stronger for the lateral trochlear inclination. Based on the adjusted *r*<sup>2</sup> value, the lateral trochlear inclination and TT–TG distance combined to account for 46 and 70 % of the variation in the lateral tilt and bisect offset index, respectively. When considering only the knee in the most extended position for each subject, which produced the largest values of lateral tilt and bisect offset index for most subjects, only the lateral trochlear inclination was significantly correlated with the bisect offset index and lateral tilt. Lateral trochlear inclination has previously been identified as a contributor to increased lateral shift and tilt of the patella at multiple flexion angles in a combination of asymptomatic subjects and subjects with patellar pain [33]. Lateral trochlear inclination has also been correlated with elevated lateral shift and tilt with the knee unloaded and extended [32]. Another study showed increased lateral tracking during extension against gravity for instability patients, compared to normal knees, but did not show a difference in the sulcus angle measured from an axial image of an MRI scan [29].

The current data did not show a significant relationship between patella alta and patellar tracking. The current study evaluated parameters based on the Insall–Salvati and Caton–Deschamps indices. Both parameters have been found to be elevated in subjects with recurrent instability [7, 34]. For studies performed with the knee loaded, elevated values for the Insall–Salvati index and Caton–Deschamps index have been associated with elevated bisect offset index and lateral patellar tilt for populations including subjects with pain [27, 33, 36], although one study indicated the lateral trochlear inclination gave the strongest correlation with bisect offset index [33]. A study evaluating unloaded knees showed significant correlations between Insall–Salvati index and bisect offset and lateral tilt, but also found the relationships were stronger for the lateral trochlear inclination [32]. Another study showed increased lateral tracking during extension against gravity for instability patients, compared to normal knees, without a difference in the Insall–Salvati index [29].

The current study included anatomical and tracking variations between subjects and between flexion angles for individual subjects. As noted for previous studies [13, 14, 29, 33, 36], patellar tilt and bisect offset index were typically largest near full extension. The lateral trochlear inclination tended to increase with increasing depth of the trochlear groove as the flexion angle increased. The TT–TG distance tended to be largest near full extension due to external rotation of the tibia emblematic of the screw home mechanism [12]. The Caton–Deschamps index tended to increase with the flexion angle

as the superior–anterior border of the tibia moved posteriorly. Variations in the anatomical parameters with the flexion angle contributed to significant correlations for the lateral trochlear inclination and TT–TG distance with tracking when considering all flexion angles. Stronger correlations occurred for the lateral trochlear inclination when considering only the most extended position for each subject, indicating the lateral trochlear inclination is the primary factor determining tracking differences between subjects.

Relative contributions of the various anatomical factors to the noted trends could be related to the anatomical abnormalities noted for the study population. The anatomical measures from the models are not identical to standard clinical measures from diagnostic images, but are similar enough for comparison. The primary differences with respect to clinical measures are related to characterizing the deepest point of the trochlear groove and the highest point on the lateral ridge of the trochlea based on interaction of the patella with the groove rather than on the outlines of the bones. For the current study, the average lateral trochlear inclination was 15° with the knee in the most extended position, when the patella was constrained by the proximal trochlear groove. Other studies have provided values for lateral trochlear inclination at the proximal trochlear groove in subjects with instability of 13° or smaller [5, 7, 26], indicating that the level of trochlear dysplasia likely was not extreme for a population of subjects with instability. The average TT–TG distance at the most extended flexion angle was 11 mm, similar to an average TT–TG distance of 12 mm with the knee extended reported for pediatric subjects with patellar instability [11], although larger values have been reported for general populations of subjects with instability [1, 7, 10, 30]. The measured TT–TG distance was likely influenced by the applied functional loading. In vitro and in vivo studies indicate that application of functional loading through the knee rotates the tibia internally at low flexion angles [19, 23], decreasing the TT–TG distance. For the current study, the average Insall–Salvati index from the most extended position of knee flexion was 1.2. Other studies have provided an Insall–Salvati index for patients with instability of 1.1–1.4 [7, 20, 21, 37], indicating that the current study group likely did not underrepresent patella alta.

The primary strengths of the study are the comparison between measures of tracking and multiple anatomical parameters related to clinical evaluation, evaluation of subjects with recurrent instability, evaluation of loaded knees at multiple flexion angles and characterizing tracking and anatomy based on 3D reconstructions. The relationships between clinically utilized parameters related to anatomy and patellar tracking can be factored into the evaluation of risk of recurrent instability and treatment planning. The close agreement between the measures made using shape matching techniques and made directly from

the low-resolution scans represents another strength. A previous study evaluating the accuracy of a similar technique for measuring patellar kinematics in comparison with Roentgen stereophotogrammetric analysis [16] showed errors on the order 1 mm and 1° for patellar shift and tilt, respectively, which are similar to the current measures of accuracy. The shape matching techniques are an important aspect of the current study due to inability to accurately identify key anatomical landmarks on models generated from the low-resolution scans in many cases.

The primary limitations of the study are related to the reduced functional capacity of the subjects and number of subjects enrolled. Due to the varying levels of pain and feelings of instability, the applied resistance to knee extension varied between subjects. Pain and feelings of instability also prevented some subjects from maintaining resisted isometric extension with the knee fully extended. The planned power of 0.8 indicates that some variables might have been significantly correlated with patellar tracking with a larger sample size, although the primary conclusion that the lateral trochlear inclination had the largest influence on tracking, with TT–TG distance as a secondary factor, would not be altered. Both clinical parameters can be used to assess the risk of lateral maltracking that can lead to recurrent instability, although the data suggests that the lateral trochlear inclination should be given primary consideration.

## Conclusion

For the pediatric population with recurrent instability evaluated for the current study, trochlear dysplasia characterized by the lateral trochlear inclination was the primary contributor to lateral maltracking during simulated functional loading. The TT–TG distance also contributed, but to a lesser extent. The anatomical measures related to lateral maltracking can help serve as indicators of the risk for continued instability and help identify surgical approaches most likely to improve patellar stability.

**Acknowledgments** Funding was provided by a research grant from the Austen BioInnovation Institute in Akron. Assistance in obtaining and exporting MRI data provided by the staff of the Department of Radiology at Akron Children's Hospital is greatly appreciated.

**Conflict of interest** The authors have no conflicts of interest related to this study.

## References

- Balcarek P, Jung K, Ammon J, Walde TA, Frosch S, Schütttrumpf JP, Stürmer KM, Frosch KH (2010) Anatomy of lateral patellar instability: trochlear dysplasia and tibial tubercle–trochlear

- groove distance is more pronounced in women who dislocate the patella. *Am J Sports Med* 38:2320–2327
2. Balcarek P, Jung K, Frosch KH, Stürmer KM (2011) Value of the tibial tuberosity–trochlear groove distance in patellar instability in the young athlete. *Am J Sports Med* 39:1756–1761
  3. Besl PJ, McKay HD (1992) A method for registration of 3-D shapes. *IEEE Trans Pattern Anal Mach Intel* 14:239–256
  4. Carpenter RD, Majumdar S, Ma CB (2009) Magnetic resonance imaging of 3-dimensional in vivo tibiofemoral kinematics in anterior cruciate ligament-reconstructed knees. *Arthroscopy* 25:760–766
  5. Carrillon Y, Abidi H, Dejour D, Fantino O, Moyon B, Tran-Minh VA (2000) Patellar instability: assessment on MR images by measuring the lateral trochlear inclination-initial experience. *Radiology* 216:582–585
  6. Cash JD, Hughston JC (1988) Treatment of acute patellar dislocation. *Am J Sports Med* 16:244–249
  7. Charles MD, Haloman S, Chen L, Ward SR, Fithian D, Afra R (2013) Magnetic resonance imaging-based topographical differences between control and recurrent patellofemoral instability patients. *Am J Sports Med* 41:374–384
  8. Cofield RH, Bryan RS (1977) Acute dislocation of the patella: results of conservative treatment. *J Trauma* 17:526–531
  9. Colvin AC, West RV (2008) Patellar instability. *J Bone Joint Surg Am* 90:2751–2762
  10. Cooney AD, Kazi Z, Caplan N, Newby M, Gibson ASC, Kader DF (2012) The relationship between quadriceps angle and tibial tuberosity–trochlear groove distance in patients with patellar instability. *Knee Surg Sports Traumatol Arthrosc* 20:2399–2404
  11. Dickens AJ, Morrell NT, Doering A, Tandberg D, Treme G (2014) Tibial tubercle–trochlear groove distance: defining normal in a pediatric population. *J Bone Joint Surg Am* 96:318–324
  12. Dietrich TJ, Betz M, Pfirrmann CW, Koch PP, Fucentese SF (2014) End-stage extension of the knee and its influence on tibial tuberosity–trochlear groove distance (TTTG) in asymptomatic volunteers. *Knee Surg Sports Traumatol Arthrosc* 22:214–218
  13. Draper CE, Besier TF, Fredericson M, Santos JM, Beaupre GS, Delp SL, Gold GE (2011) Differences in patellofemoral kinematics between weight-bearing and non-weight-bearing conditions in patients with patellofemoral pain. *J Orthop Res* 29:312–317
  14. Draper CE, Besier TF, Santos JM, Jennings F, Fredericson M, Gold GE, Beaupre GS, Delp SL (2009) Using real-time MRI to quantify altered joint kinematics in subjects with patellofemoral pain and to evaluate the effects of a patellar brace or sleeve on joint motion. *J Orthop Res* 27:571–577
  15. Faul F, Erdfelder E, Buchner A, Lang A-G (2009) Statistical power analyses using G\*Power 3.1: tests for correlation and regression analyses. *Behav Res Methods* 41:1149–1160
  16. Fellows RA, Hill NA, Gill HS, MacIntyre NJ, Harrison MM, Ellis RE, Wilson DR (2005) Magnetic resonance imaging for in vivo assessment of three-dimensional patellar tracking. *J Biomech* 38:1643–1652
  17. Fithian DC, Paxton EW, Stone ML, Silva P, Davis DK, Elias DA, White LM (2004) Epidemiology and natural history of acute patellar dislocation. *Am J Sports Med* 32:1114–1121
  18. Hopper GP, Leach WJ, Rooney BP, Walker CR, Blyth MJ (2014) Does degree of trochlear dysplasia and position of femoral tunnel influence outcome after medial patellofemoral ligament reconstruction? *Am J Sports Med* 42:716–722
  19. Johal P, Williams A, Wragg P, Hunt D, Gedroyc W (2005) Tibiofemoral movement in the living knee. A study of weight bearing and non-weight bearing knee kinematics using ‘interventional’ MRI. *J Biomech* 38:269–276
  20. Kepler CK, Bogner EA, Hammoud S, Malcolmson G, Potter HG, Green DW (2011) Zone of injury of the medial patellofemoral ligament after acute patellar dislocation in children and adolescents. *Am J Sports Med* 39:1444–1449
  21. Kita K, Horibe S, Toritsuka Y, Nakamura N, Tanaka Y, Yonetani Y, Mae T, Nakata K, Yoshikawa H, Shino K (2012) Effects of medial patellofemoral ligament reconstruction on patellar tracking. *Knee Surg Sports Traumatol Arthrosc* 20:829–837
  22. Lewallen LW, McIntosh AL, Dahm DL (2013) Predictors of recurrent instability after acute patellofemoral dislocation in pediatric and adolescent patients. *Am J Sports Med* 41:575–581
  23. Li G, Rudy TW, Sakane M, Kanamori A, Ma CB, Woo SL (1999) The importance of quadriceps and hamstring muscle loading on knee kinematics and in situ forces in the ACL. *J Biomech* 32:395–400
  24. Maenpaa H, Lehto MU (1997) Patellar dislocation. The long-term results of nonoperative management in 100 patients. *Am J Sports Med* 25:213–217
  25. McWalter EJ, Hunter DJ, Harvey WF, McCree P, Hirko KA, Felson DT, Wilson DR (2011) The effect of a patellar brace on three-dimensional patellar kinematics in patients with lateral patellofemoral osteoarthritis. *Osteoarthritis Cartil* 19:801–808
  26. Nelitz M, Theile M, Dornacher D, Wölfe J, Reichel H, Lipbacher S (2012) Analysis of failed surgery for patellar instability in children with open growth plates. *Knee Surg Sports Traumatol Arthrosc* 20:822–828
  27. Pal S, Besier TF, Beaupre GS, Fredericson M, Delp SL, Gold GE (2013) Patellar maltracking is prevalent among patellofemoral pain subjects with patella alta: an upright, weightbearing MRI study. *J Orthop Res* 31:448–457
  28. Pennock AT, Alam M, Bastrom T (2014) Variation in tibial tubercle–trochlear groove measurement as a function of age, sex, size, and patellar instability. *Am J Sports Med* 42:389–393
  29. Regalado G, Lintula H, Eskelinen M, Kokki H, Kröger H, Svedström E, Vahlberg T, Väättäin U (2014) Dynamic KINE-MRI in patellofemoral instability in adolescents. *Knee Surg Sports Traumatol Arthrosc*. doi:10.1007/s00167-013-2679-5
  30. Schoettle PB, Zanetti M, Seifert B, Pfirrmann CW, Fucentese SF, Romero J (2006) The tibial tuberosity–trochlear groove distance: a comparative study between CT and MRI scanning. *Knee* 13:26–31
  31. Stefanik JJ, Roemer FW, Zumwalt AC, Zhu Y, Gross KD, Lynch JA, Frey-Law LA, Lewis CE, Guermazi A, Powers CM, Felson DT (2012) Association between measures of trochlear morphology and structural features of patellofemoral joint osteoarthritis on MRI: the MOST study. *J Orthop Res* 30:1–8
  32. Stefanik JJ, Zumwalt AC, Segal NA, Lynch JA, Powers CM (2013) Association between measures of patella height, morphologic features of the trochlea, and patellofemoral joint alignment: the MOST study. *Clin Orthop Relat Res* 471:2641–2648
  33. Teng HL, Chen YJ, Powers CM (2014) Predictors of patellar alignment during weight bearing: an examination of patellar height and trochlear geometry. *Knee* 21:142–146
  34. Tsuda E, Ishibashi Y, Yamamoto Y, Maeda S (2012) Incidence and radiologic predictor of postoperative patellar instability after Fulkerson procedure of the tibial tuberosity for recurrent patellar dislocation. *Knee Surg Sports Traumatol Arthrosc* 20:2062–2070
  35. Varadarajan KM, Freiberg AA, Gill TJ, Rubash HE, Li G (2010) Relationship between three-dimensional geometry of the trochlear groove and in vivo patellar tracking during weight-bearing knee flexion. *J Biomech Eng* 132:061008
  36. Ward SR, Terk MR, Powers CM (2007) Patella alta: association with patellofemoral alignment and changes in contact area during weight-bearing. *J Bone Joint Surg Am* 89:1749–1755
  37. Yamada Y, Toritsuka Y, Yoshikawa H, Sugamoto K, Horibe S, Shino K (2007) Morphological analysis of the femoral trochlea in patients with recurrent dislocation of the patella using three-dimensional computer models. *J Bone Joint Surg Br* 89:746–751